

DOI:10.11835/j.issn.2096-6717.2020.082

开放科学(资源服务)标识码(OSID):



Transparent soil model testing on ground settlement induced by parallel tunnels excavation

LIU Hanlong^{a,b,c}, ZHONG Haiyi^b, GU Xin^b, XIANG Yuzhou^b, ZHANG Wengang^{a,b,c}

(a. Key Laboratory of New Technology for Construction of Cities in Mountain Area, Ministry of Education; b. School of Civil Engineering, c. National Joint Engineering Research Center of Geohazards Prevention in the Reservoir Areas; Chongqing University, Chongqing 400045, P. R. China)

Abstract: Parallel tunnels are generally constructed in urban subways to facilitate the movement of traffic in modern cities. Common solutions for predicting settlement induced by the excavation of two parallel tunnels are based on the single tunnel case and the simplified superposition method is utilized to generate the deformation profile without considering the interaction between the two tunnels. In this study, transparent soil model tests were performed to visualize the surface and subsurface settlement induced by the excavation of two parallel tunnels in sandy ground. Several key factors influencing the interaction of the parallel tunnels, as well as the surface and subsurface settlement, were investigated, including the spacing between the two tunnels, the volume of ground loss and the depth at which the tunnels were buried. Then the relationship between volume of the ground loss and the settlement was established. It is hoped that this study can provide guidelines for the design and construction of urban parallel tunnels excavations.

Keywords: transparent soil; parallel tunnels; model test; surface settlement; subsurface settlement

平行隧道开挖引起场地沉降的透明土模型试验研究

刘汉龙^{a, b, c}, 钟海怡^b, 顾鑫^b, 向钰周^b, 仇文岗^{a, b, c}

(重庆大学 a. 山地城镇建设与新技术教育部重点实验室; b. 土木工程学院; c. 库区环境地质灾害防治国家地方联合工程研究中心, 重庆 400045)

摘要:为了便捷现代城市交通,地铁系统普遍采用平行隧道模式。平行隧道开挖引起的场地沉降预测一般基于单一隧道工况,利用简化叠加法生成变形剖面,而没有考虑两个隧道之间的相互作用。采用透明土模型试验技术,自主研发平行隧道模型试验装置及试验方法,研究了在砂质场地上开挖平行隧道引起的地表和地层沉降特性。通过模型试验探索了平行隧道间距、土体损失率、埋深等要素对地表和地表沉降的影响规律。在此基础上,量化了土体损失率和场地沉降值间的数值关系。此数值关系可为砂质场地中平行隧道施工与设计提供参考依据,也为隧道间距初选以及埋深的初步确定提供理论支撑。

关键词:透明土;平行隧道;模型试验;地表沉降;地层沉降

中图分类号:TU411.93 **文献标志码:**A **文章编号:**2096-6717(2021)01-0001-10

Received: 2020-05-16

Foundation items: Chongqing Construction Science and Technology Plan Project (No. 2019-0045); Fundamental Research Funds for the Central Universities (No. 2019CDJDTM0007); Graduate Research and Innovation Foundation of Chongqing (No. CYS18024)

Author brief: LIU Hanlong (1964-), professor, doctoral supervisor, main research interest: geotechnical engineering, hliuhhu@163.com.

ZHANG Wengang (corresponding author), professor, doctoral supervisor, E-mail zhangwg@cqu.edu.cn.

1 Introduction

With the rapid development of the modern city, burying the subway tunnels has proven to be an effective way to relieve traffic pressure on the ground. Accurate estimation of ground settlement is vital to ensure safety during the tunnel excavation. To this end, many early scholars have studied both the surface and the subsurface settlement for the excavation of the single tunnel^[1-4]. However, single tunnel construction is rarely encountered in practice. Instead, parallel tunnels excavated sequentially are commonly constructed in urban subways to facilitate the movement of traffic in modern cities. In comparison to monitoring the deformation in clays^[1-2], the settlement caused by tunneling in granular soils (e. g. , sands and gravels) are more difficult and complex when considering key factors such as the relative density, which influences the shape and magnitude of the deformation^[5]. Recently, the settlement of single tunnels in sand has been studied through model testing^[6] and numerical simulation^[7-8]. Yet the deformation induced by sequential excavation of parallel tunnels has not been fully revealed. Therefore, it may be a research hotspot in geotechnical engineering to investigate the deformation induced by the excavations of two parallel tunnels.

Many studies based on analytical deduction have been carried out to investigate the deformation induced by tunnel excavation, but they mainly aimed at the single tunnel^[9-13]. Parallel-tunneling deformation prediction generally utilizes the simplified superposition method with the assumption the deformation arising from the excavation of the 2nd tunnel is unaffected by that of the 1st tunnel. However, previous research, particularly numerical studies that can fully consider the interaction between two tunnels, have indicated that this method may not be directly applicable to estimating the parallel tunneling-

induced settlement in practice, since it may underestimate the resultant settlement, which may exert a negative effect on the safety of the nearby constructions^[14]. The numerical simulation of tunneling which permits calculating internal soil deformation is widely used in the last decade^[14-18]. However, not only is internal soil deformation difficult to validate against the actual measurements, but the key input parameters, which can directly and significantly impact the accuracy of the results, are quite difficult to obtain. Many scholars have focused on in-situ surface settlement induced by sequential excavation of parallel tunnels in a variety of soils. Since the in-situ test is costly and time-consuming, laboratory tests are widely used in performing two-dimensional trap door tests in dry sand^[19] and lining installation in a centrifuge^[20-21]. However, it is challenging to obtain the inner soil deformation and the failure pattern from the conventional model tests. Moreover, the results from traditional laboratory test are inevitably affected by the boundary conditions and the embedment of the rigid sensors has an effect on instrumentation accuracy due to the arching effect^[22-23]. Recently the development of data-driven and soft computing methods, Zhang et al.^[24-25] and Shahrour and Zhang^[26] predicted the surface settlement induced by earth pressure balance shield tunneling, estimated the lining response for twin-tunnel construction, and performed TBM tunneling optimization. However, this kind of data-based method has an obvious deficiency in revealing the deformation characteristics in tunneling constructions, where the internal physical failure mechanism is often ignored.

To visualize the interior or the full-field deformation, an advanced modeling technique using the transparent soil is adopted in this study, which was firstly developed by Allersma^[27] and utilized by many scholars worldwide^[28-29], including in tunneling by Ahmed and Iskander^[30-31]. And the intend of this paper is to explore the parallel-tunnel

interaction and its influence on surface and subsurface settlements due to the second tunnel in sandy ground considering the spacing (S) between two tunnels, the magnitude of the volume of ground loss at the tunnel (V_1) and burial depth (H and H_0).

2 Experimental design

2.1 Testing apparatus

The model testing system was adopted to monitor the settlement variation during excavation. It consisted of a computer, an optical platform, a charge coupled device (CCD) camera, a disk laser, a plexiglass model tank, and processing software for particle image velocimetry (PIV) digital images. The optical platform was ferromagnetic stainless steel and the inner core structure on the top side offered considerable anti-disturbance capacity. The high resolution of the CCD camera was 1280×960 pixels, which could record the settlement during tunnel excavation continuously operated by the control program of the computer. The disk laser was EP532-3W along with 3 W output power, 532 nm wavelength, 10° - 25° light angle and less than 1 mm thickness. The multifunctional model box made of acrylic plexiglass with each surface bonded by strong glue was capable of simulating the single tunnel test, parallel tunnels test and cross tunnels test, for a total of four tunnels (three on the front and one on the side). Additionally, ribs were fixed at the bottom to restrain the deformation.

2.2 Testing materials

Fused silica sand, which has similar physical and mechanical properties to the proxy naturally graded sand, was adopted in this study to manufacture the transparent soil samples. The particles were 0.5-1.0 mm in size. The maximum dry density was 1.278 g/cm^3 , and the minimum was 0.907 g/cm^3 . The relative density was 55% and the internal friction angle was between 34° and 38° . The pore liquid was mixed with n-dodecane and the 15th mineral white oil with the mass ratio

of 1:4 and its refractive index was 1.4585. The periphery of the tunnel was isolated from the surrounding soil with a self-made film tube made of transparent and highly elastic thermoplastic polyurethane (TPU) film to prevent the pore liquid from flowing out along the tunnel model hole during the test. The drainage method was used to simulate the tunnel excavation process. One end of a rubber tube with a diameter of 50 mm was tied with a wire, and the other end was sleeved on a rubber plug with a drainage tube and tied with a rubber band to prevent potential water leakage. Before the test, the model box was cleaned, and the tunnel model, as well as the waterproof film tube, was set up.

To prepare the transparent soil, marks were made every 10 mm along the vertical direction of the model box, then the volume of 10 mm thickness of the transparent soil was calculated as the unit volume and the weight of the fused silica and the amount of drainage for the unit volume were determined. The prepared mixed oil was slowly poured into the model box and then the weighed fused silica sand was uniformly poured into the model box and the mixed oil and the silica sand were mixed together. During the configuration process, the transparent soil was slowly stirred with a glass rod to eliminate the air bubbles. Then, the stratified compaction method (each layer was 10 mm thick) was used to make it satisfy the required target density. Finally, the load 1 000 kN was exerted on the prepared transparent soil for 24 hours to ensure that the relative density was constant.

2.3 Testing process

The PIV post-processing program was used to obtain the displacement from pictures during the test^[32-33]. The volume of the settlement trough was directly measured by importing the experimental results into AutoCAD software according to the displacement curve of the settlement point. The stability of the sand after excavation is poor and it is difficult to form an arch. Therefore, it can be

assumed that the drainage volume is equal to the convergence value around the tunnel, indicating that the volume of soil loss is equal to the volume of drainage.

The total liquid volume is $V_w = 687$ mL. There are totally 10 times of drainage for the simulation of incremental tunnel excavation. The drainage volume is 10 mL for each time. Prior to the test, place the model box in a suitable position, put the camera right beside the model box aiming at the center of its cross section then adjust their relative position to make the image clear. Adjust the laser intensity to ensure the figure from the transparent soil form a stable and clear bright spot. TA (Tunnel A) and TB (Tunnel B) are excavated sequentially via draining the liquid in the rubber tube and every excavation footage length is $0.5D$ (tunnel diameter). The laser position should be moved along the sliding rail accordingly with the excavation footage.

2.4 Key influential parameters and testing schemes

For both surface settlement and subsurface settlement, six tests, divided into two groups, were performed (shown in Table 1). Group 1 and Group 2 each consisted of three tests to investigate the effects of the volume of ground loss at tunnel (V_1), burial depth (H and H_0) and tunnel spacing (S) on the twin-tunnel-induced surface and subsurface settlement. The size of the model box is plotted in Fig. 1, where $F = 1\ 600$ N. Fig. 2 presents the cross-section diagram of the settlement trough and parts of the related parameters.

Table 1 Model Testing Scheme

(a) Testing scheme for surface settlement

Group	Test ID	H/D	S/D
1	T1	2	1.5
	T2	2	2.0
	T3	2	4.5
2	T4	5	1.5
	T5	5	2.0
	T6	5	4.5

(b) Testing scheme for subsurface settlement

Group	Test ID	H_0/D	H/D	S/D
1	U1	1	5	1.5
	U2	2	5	1.5
	U3	4	5	1.5
2	U4	1	5	4.5
	U5	2	5	4.5
	U6	4	5	4.5

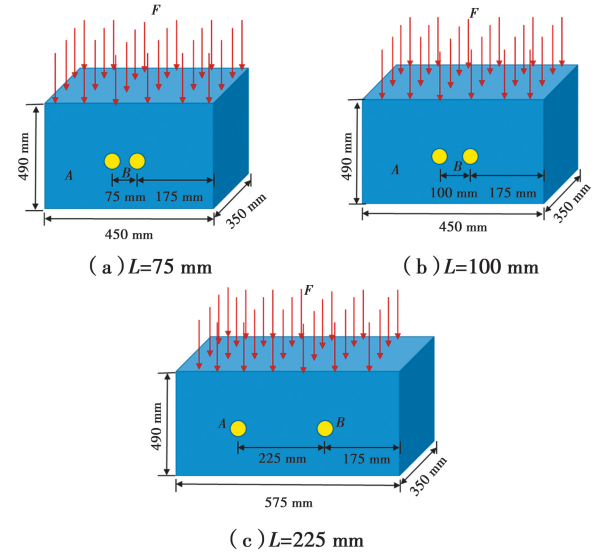


Fig. 1 Schematic diagram for model dimensions and boundary conditions

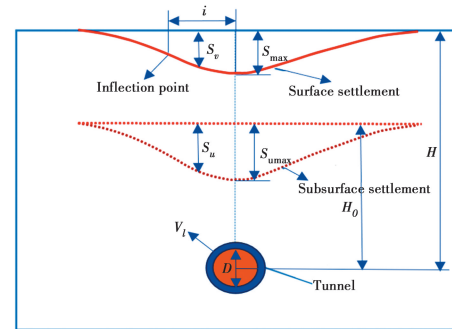


Fig. 2 Cross-sectional diagram of the settlement trough and relevant parameters

3 Testing result and analysis

3.1 Surface settlement

3.1.1 Surface settlement due to excavation of the 1st tunnel

Fig. 3 presents the measured surface settlement S_{V_A} induced by TA under H (Depth from the surface to the tunnel axis level)/ $D=2.0$

and 5.0, respectively. The normal probability Gaussian curves proposed by Peck^[3] were used to fit the measured data. The surface settlement of the 1st tunnel excavation has good agreement with O'Reilly and New^[2], which is expected since TA is excavated in a greenfield site and this behavior is reflected in the first tunnel settlement for all tests. Moreover, the Gaussian curves give a good fit when $V_1=1.455\%$ and 2.911% , then the goodness of the fit declines with the increase in V_1 , which coincides with the observations by Marshall et al. ^[5].

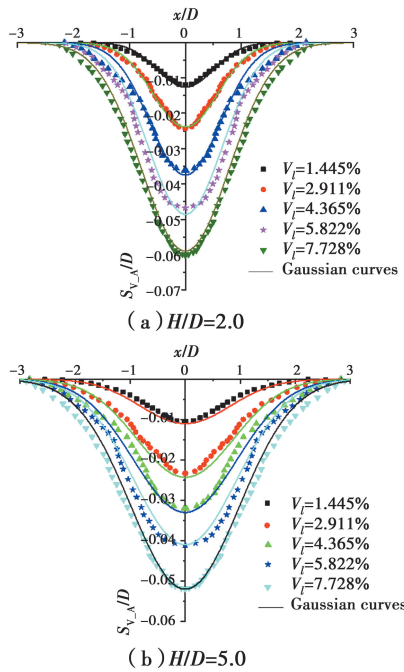


Fig. 3 Gaussian curve fitting to the surface settlement induced by the TA under different H/D values

As seen in Fig. 4 (a), the maximum surface settlement S_{\max_A} linearly increases with V_1 , which can also be seen in Shahin et al. ^[34]. From Fig. 4 (b), the soil volume loss of surface settlement V_{S_A} is smaller than V_1 in all performed tests, especially at large V_1 and H which is in good agreement with Zheng et al. ^[35], who points out that the soil within the subsurface ground may exhibit an overall dilating response considering that the tests were conducted in a low-stress condition.

3.1.2 Surface settlement due to excavation of the 2nd tunnel

The resultant surface settlement S_V of

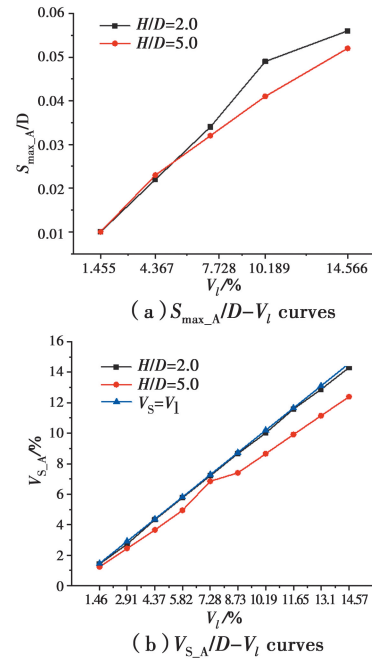


Fig. 4 Variations of S_{\max_A}/D and V_{S_A} with V_1

different groups is plotted in Fig. 5. Fundamentally, the distribution of the resultant ground settlement under $H/D = 2.0$ and 5.0 changes from a “V” shape to a “W” shape step by step as S becomes larger.

From Fig. 5, it is clear that the position corresponding to S_{\max_A} is directly above TA during the tunnel excavation of TA. With the increase of V_1 in TB, the position corresponding to S_{\max_B} gradually moves towards the axis of TB and the asymmetry of the settlement trough becomes more significant in T1, T2, T3 and T4 ($S=1.5D$ and $2.0D$). But for the tests (T3 and T6) that have larger S , the position corresponding to S_{\max_B} is also just above TB, which means the excavation of TA has little influence on TB.

From Fig. 6, it is clear that for T1, T2, T4 and T5, the corresponding location of the maximum surface settlement X moves toward TB as V_1 increases and the asymmetry of the settlement trough also becomes more significant. For T3, the corresponding locations of the maximum surface settlement X remains constant and the excavation of TA has little impact on TB. For T4, although X does not change, the settlement trough curves appear as an inflection point at $X=1.5D$.

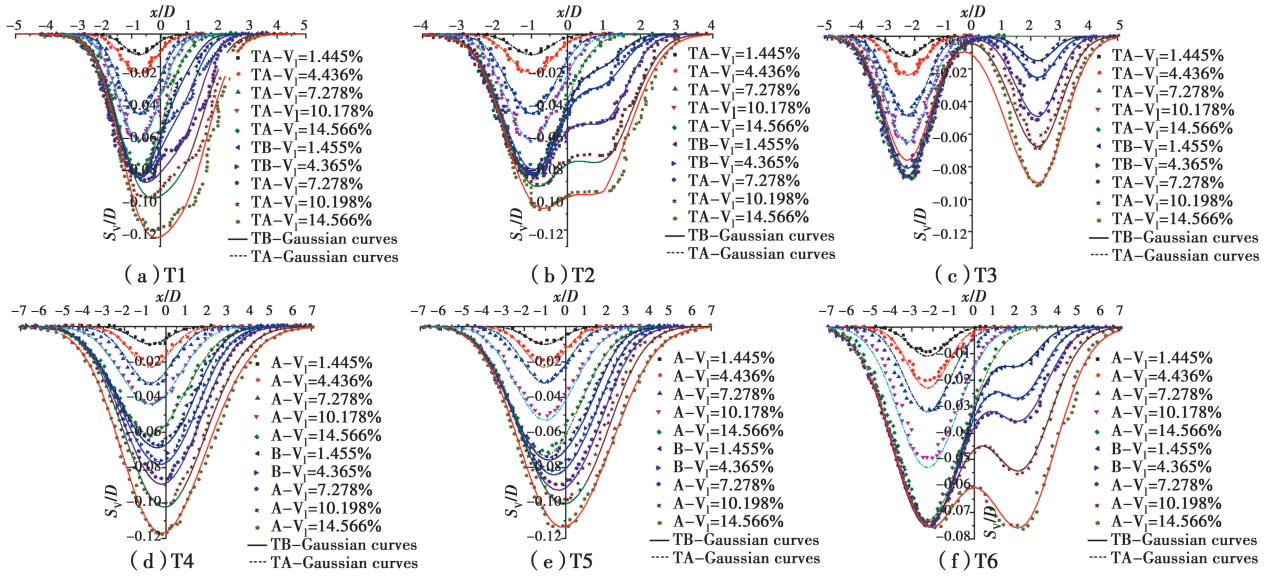


Fig. 5 Surface settlement of TA and TB for different ground volume losses

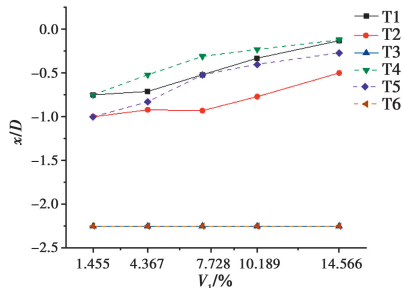


Fig. 6 Variations in X/D with different V_1

To further investigate the settlement caused by each excavation, the net surface settlement $S_{v,B}$ induced by TB is shown in Fig. 7. The settlement of TB is obtained from the resultant ground settlement subtracting the 1st tunnel settlement. Gaussian curves are again used to fit the experimental data. The goodness-of-fit of the Gaussian curves is shown to decrease with the development of V_1 in the TB excavation, which is similar to the observations in the TA excavation.

Fig. 8(a) shows the $S_{\max,B}/D-V_1$ curves gained from the six tests. Basically, a non-linear relationship is found between $S_{\max,B}$ and V_1 . $S_{\max,B}$ grows up gradually as V_1 developed. Moreover, its magnitude is larger compared with $S_{\max,A}$ as plotted in Fig. 3, which is consistent with the conclusion obtained in clayey soils that the larger settlement in the 2nd tunnel excavation is caused by the interaction between the two tunnels^[36-37].

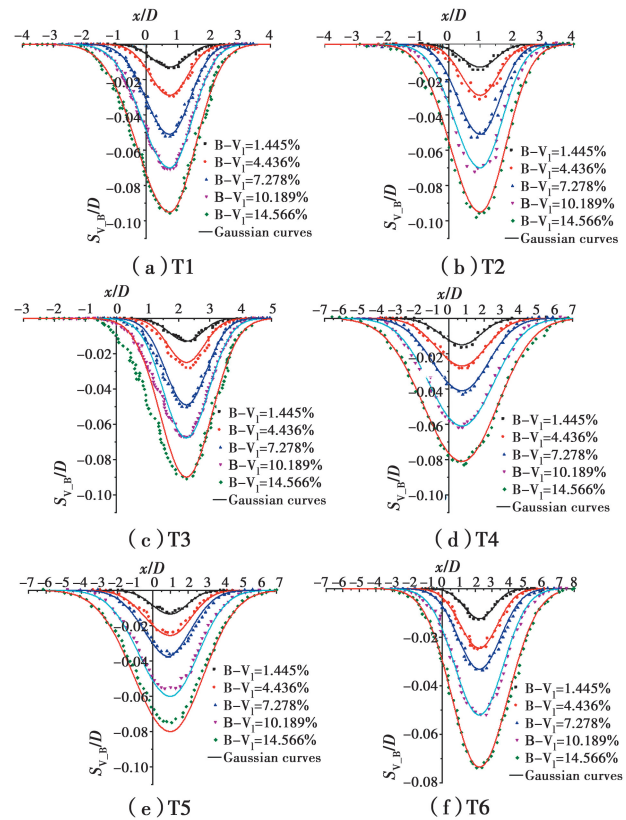


Fig. 7 Gaussian curve fitting to the surface settlement induced by TB

To further illustrate the impact of parallel-tunnel interaction on $S_{\max,B}$, variations in $S_{\max,B}/S_{\max,A}$ with different V_1 are plotted in Fig. 8(b). Basically, S appears to be the most dominant factor influencing the values of $S_{\max,B}/S_{\max,A}$. The influence of the twin-tunnel interaction is more

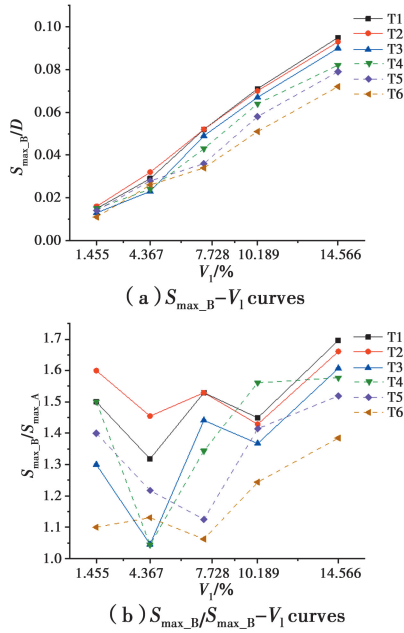


Fig. 8 Variations of S_{\max_B} and S_{\max_B}/S_{\max_A} with V_1

significant in T1, T2, T4 and T5 ($S=1.5D$ and $2.5D$), than in T3 and T6 ($S=4.5D$) as well as in the case of smaller H ($H=2D$).

Fig. 9 presents the values of the empirical coefficient for surface settlement k under different V_1 for different H/D . Here, k_l and k_r represent the empirical coefficients of the left and right sides of the settlement trough, respectively. k gradually increases with V_1 under the same S . Conversely, it decreases step by step with the increase of S . Moreover, k_l gets closer to k_r as S increases, indicating that both sides of the settlement trough tend to be symmetrical.

3.2 Subsurface settlement

The resultant subsurface settlement S_u of different groups is plotted in Fig. 10. Basically, the distribution of Group 1 gradually changes from a “W” shape to a “V” shape as H_0 (Depth from the subsurface to the tunnel axis level)/ D becomes larger. And the distribution of Group 2 remains in the shape of a “W”. From Fig. 11, it is clear that for Group 1, the corresponding location of the maximum subsurface settlement X_u moves toward TB as V_1 increases. The asymmetry of the settlement trough for U1 and U2 becomes more significant, while for U3, the curves of the

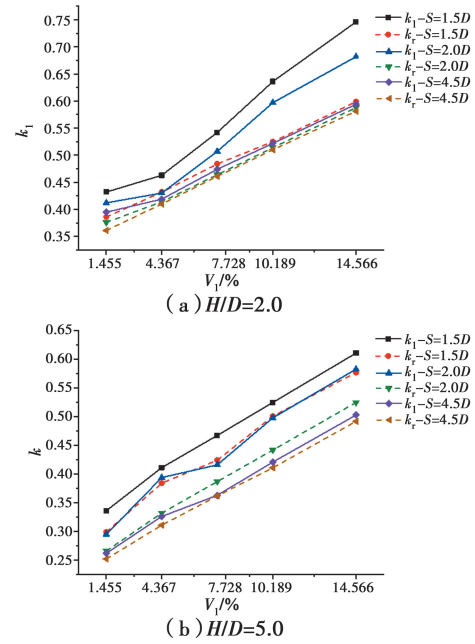


Fig. 9 Variations of k with different V_1 for $H/D=2.0$ and 5.0

settlement trough undergo a process from asymmetry to symmetry and then back to asymmetry. As for Group 2, X_u is also just above TB and their settlement trough curves are quite similar, which means the excavation of TA has little influence on TB.

4 Summary and conclusions

Based upon the surface and subsurface settlements observed during the transparent soil model test, some useful conclusions are drawn as shown below:

1) With the increase of the ground volume loss, the Gaussian curve used to predict the ground settlement induced by the excavation of the two parallel tunnels demonstrates a decreasing trend.

2) The interaction of the parallel tunnels leads to greater maximum surface settlement S_{\max_B} during the excavation of TB compared with that of TA. This effect weakens as the spacing between the parallel tunnels increases.

3) When $S=1.5D$ and $2.0D$, the excavation of the 1st tunnel has a significant effect on the surface settlement of the 2nd tunnel, and the corresponding location of S_{\max} gradually moves towards the axis of the 2nd tunnel with the increase

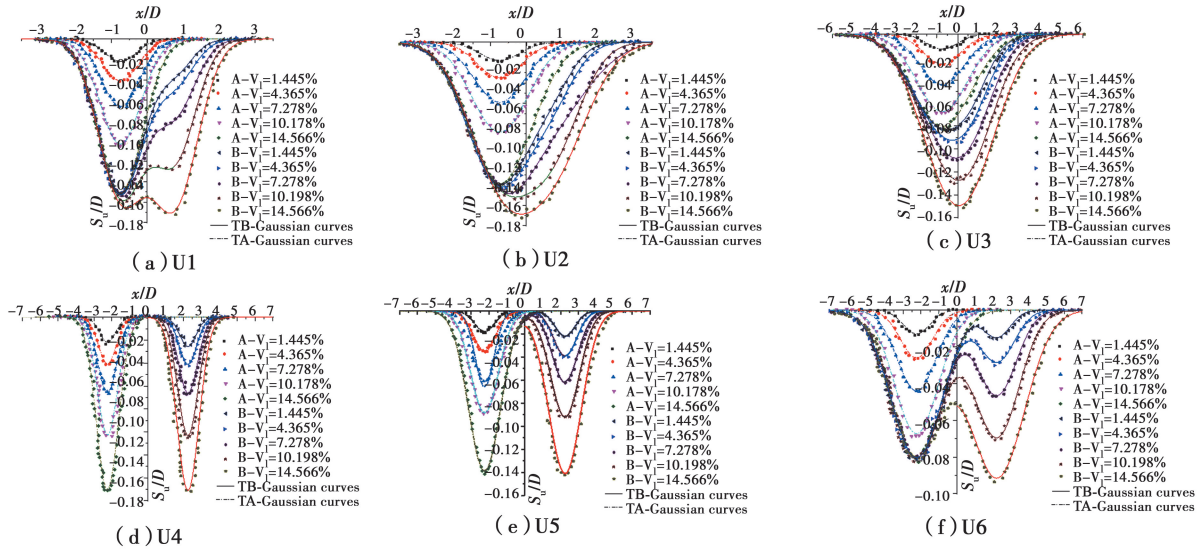


Fig. 10 Subsurface settlement of TA and TB for different ground volume losses

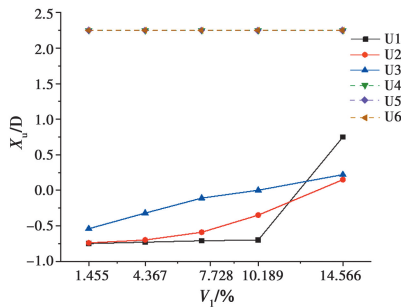


Fig. 11 Variations of X_u/D with different V_1

of V_1 . Moreover, the asymmetry of the settlement trough becomes more obvious. When $S = 4.5D$, the excavation of the 1st tunnel has a marginal influence on the deformation of the 2nd tunnel.

4) Under the same S , k gradually increases with the growth of V_1 while it declines as S develops. The empirical coefficients k of the left and right sides get closer as S increases.

Acknowledgements

The authors would like to acknowledge the financial support from the Chongqing Construction Science and Technology Plan Project (No. 2019-0045), Fundamental Research Funds for the Central Universities (No. 2019CDJDTM0007) and the Graduate Research and Innovation Foundation of Chongqing (Grant No. CYS18024).

References:

[1] MAIR R J, TAYLOR R N, BRACEGIRDLE A. Subsurface settlement profiles above tunnels in clays [J]. Geotechnique, 1993, 43(2): 315-320.

[2] O'REILLY M P, NEW B M. Settlements above tunnels in the United Kingdom - Their magnitudes and prediction [C]//Proceedings of Tunnelling '82 Symposium, Springer, Berlin, 1982; 173-181.

[3] PECK R B. Deep excavations and tunneling in soft ground [C]//Proceedings of the Seventh International Conference on Soil Mechanics and Foundation Engineering, Mexico, Balkema, 1969, 3: 225-290.

[4] SCHMIDT B. Settlement and ground movement associated with tunneling in soils [D]. Urbana: University of Illinois, 1969.

[5] MARSHALL A M, FARRELL R P, KLAR A, et al. Tunnels in sands: the effect of size, depth and volume loss on greenfield displacements [J]. Geotechnique, 2012, 62(5): 385-399.

[6] FRANZA A, ZHOU B, MARSHALL A M. The effects of relative tunnel depth and volume loss on vertical settlements above tunnels in dense sands [C]//Fourth Geo-China International Conference. July 25-27, 2016, Shandong, China. Reston, VA, USA: American Society of Civil Engineers, 2016: 125-132.

[7] YANG B W, BLOODWORTH A. Numerical analysis of tunnelling in sand-A case study of a centrifuge test [C]//Proceedings of GeoShanghai 2018 International Conference: Tunnelling and Underground Construction, 2018.

[8] ZHOU B, ELKAYAM I, MARSHALL A. The effect

- of relative density on tunnelling-induced settlements - DEM simulations versus centrifuge test results[M]// Geomechanics from Micro to Macro. CRC Press, 2014: 589-594.
- [9] BOBET A. Analytical solutions for shallow tunnels in saturated ground [J]. *Journal of Engineering Mechanics*, 2001, 127(12): 1258-1266.
- [10] CHI S Y, CHERN J C, LIN C C. Optimized back-analysis for tunneling-induced ground movement using equivalent ground loss model [J]. *Tunnelling and Underground Space Technology*, 2001, 16 (3): 159-165.
- [11] CHOU W I, BOBET A. Predictions of ground deformations in shallow tunnels in clay [J]. *Tunnelling and Underground Space Technology*, 2002, 17(1): 3-19.
- [12] PARK K H. Analytical solution for tunnelling-induced ground movement in clays [J]. *Tunnelling and Underground Space Technology*, 2005, 20 (3): 249-261.
- [13] VERRUIJT A, BOOKER J R. Surface settlements due to deformation of a tunnel in an elastic half plane [J]. *Géotechnique*, 1996, 46(4): 753-756.
- [14] ADDENBROOKE T, POTTS D M. Twin tunnel interaction: surface and subsurface effects [J]. *International Journal of Geomechanics*, 2001, 1(2): 249-271.
- [15] GONZÁLEZ N A, ROUAINIA M, ARROYO M, et al. Analysis of tunnel excavation in London Clay incorporating soil structure [J]. *Géotechnique*, 2012, 62(12): 1095-1109.
- [16] KASPER T, MESCHKE G. A 3D finite element simulation model for TBM tunnelling in soft ground [J]. *International Journal for Numerical and Analytical Methods in Geomechanics*, 2004, 28(14):1441-1460.
- [17] ZHANG W G, ZHANG R H, WU C Z, et al. State-of-the-art review of soft computing applications in underground excavations [J]. *Geoscience Frontiers*, 2020, 11(4): 1095-1106.
- [18] CHEN F Y, WANG L, ZHANG W G. Reliability assessment on stability of tunnelling perpendicularly beneath an existing tunnel considering spatial variabilities of rock mass properties [J]. *Tunnelling and Underground Space Technology*, 2019, 88: 276-289.
- [19] VARDOULAKIS I, GRAF B, GUDEHUS G. Trap-door problem with dry sand: A statical approach based upon model test kinematics [J]. *International Journal for Numerical and Analytical Methods in Geomechanics*, 1981, 5(1): 57-78.
- [20] CHAPMAN D N, AHN S K, HUNT D V L, et al. The use of model tests to investigate the ground displacements associated with multiple tunnel construction in soil [J]. *Tunnelling and Underground Space Technology*, 2006, 21(3/4): 413.
- [21] KIM S H. Interaction between closely spaced tunnels in clay [D]. Oxford, UK: Oxford University, 1996: 242.
- [22] LEE C J, CHIANG K H, KUO C M. Ground movement and tunnel stability when tunneling in sandy ground [J]. *Journal of the Chinese Institute of Engineers*, 2004, 27(7): 1021-1032.
- [23] XIANG Y Z, LIU H L, ZHANG W G, et al. Application of transparent soil model test and DEM simulation in study of tunnel failure mechanism [J]. *Tunnelling and Underground Space Technology*, 2018, 74: 178-184.
- [24] ZHANG W G, LI H R, WU C Z, et al. Soft computing approach for prediction of surface settlement induced by earth pressure balance shield tunneling [J/OL]. *Underground Space*, 2020. <https://doi.org/10.1016/j.undsp.2019.12.003>.
- [25] ZHANG W G, LI Y Q, WU C Z, et al. Prediction of lining response for twin tunnels constructed in anisotropic clay using machine learning techniques [J/OL]. *Underground Space*, 2020. DOI: 10.1016/j.undsp.2020.02.007.
- [26] SHAHROUR I, ZHANG W G. Use of the soft computing techniques for TBM tunnelling optimization [J/OL]. *Underground Space*, 2020. <https://doi.org/10.1016/j.undsp.2019.12.001>
- [27] ALLERSMA H. Photo-elastic stress analysis and strains in simple shear[C]//Proc. Iutam Symposium on Deformation and Failure of Granular Materials, 1982: 345-353.
- [28] CAI M, KAISER P K, MORIOKA H, et al. FLAC/PFC coupled numerical simulation of AE in large-scale underground excavations [J]. *International Journal of Rock Mechanics and Mining Sciences*, 2007, 44(4): 550-564.
- [29] NG C W W, SHI J W, HONG Y. Three-dimensional centrifuge modelling of basement excavation effects on an existing tunnel in dry sand [J]. *Canadian Geotechnical Journal*, 2013, 50(8): 874-888.
- [30] AHMED M, ISKANDER M. Evaluation of tunnel face stability by transparent soil models [J]. *Tunnelling and*

- Underground Space Technology, 2012, 27 (1): 101-110.
- [31] AHMED M, ISKANDER M. Analysis of tunneling-induced ground movements using transparent soil models [J]. Journal of Geotechnical and Geoenvironmental Engineering, 2011, 137 (5): 525-535.
- [32] LIU J Y. Visualizing 3-D internal soil deformation using laser speckle and transparent soil techniques [C]//GeoHunan International Conference 2009. August 3-6, 2009, Changsha, Hunan, China. Reston, VA, USA: American Society of Civil Engineers, 2009: 123-128.
- [33] SADEK S, ISKANDER M, LIU J Y. Geotechnical properties of transparent silica [J]. Canadian Geotechnical Journal, 2002, 39(1): 111-124.
- [34] SHAHIN H M, NAKAI T R, ZHANG F, et al. Behavior of ground and response of existing foundation due to tunneling [J]. Soils and Foundations, 2011, 51 (3): 395-409.
- [35] ZHENG G, TONG J B, ZHANG T Q, et al. Experimental study on surface settlements induced by sequential excavation of two parallel tunnels in drained granular soil [J]. Tunnelling and Underground Space Technology, 2020, 98: 103347.
- [36] CHAPMAN D, AHN S K, HUNT D V L. Investigating ground movements caused by the construction of multiple tunnels in soft ground using laboratory model tests [J]. Canadian Geotechnical Journal, 2007, 44(6): 631-643.
- [37] DIVALL S, GOODEY R J. Twin-tunnelling-induced ground movements in clay [J]. Proceedings of the Institution of Civil Engineers-Geotechnical Engineering, 2015, 168(3): 247-256.

(编辑 胡英奎)